August 27-31, 2023
FLORENCE - ITALY
ICWE 16
16th International Conference on Wind Engineering

Experimental investigation on wind-induced vibration of photovoltaic modules supported by suspension cables

Haiwei XU [1], Kunyang DING [1], Guohui SHENG [1]

[1] *College of Civil Engineering and Architecture, Zhejiang University, Hangzhou, 310058, China, Email address: haiweix@zju.edu.cn*

SUMMARY:
Aeroelastic wind tunnel test and rigid model wind tunnel test were conducted on a large-span cable supported photovoltaic module with tilt angles of 0° and 10°, respectively. The effects of tilt angle, cable pretension and wind speed on the wind-induced response and the aerodynamic damping of the photovoltaic module are analyzed. Based on the wind pressure test of the rigid model, the three-dimensional wind-induced vibration characteristics of the photovoltaic module were investigated using finite element simulation techniques. The wind vibration coefficients of the photovoltaic modules with a tilt angle of 10° were estimated from multi-target equivalent static wind loads. The study result shows that wind-induced vertical vibration of the photovoltaic module increases with tilt angle, but reduces with increase of cable pretension. The root mean square of vertical displacement shows an almost linear increase with square of wind speed. Negative aerodynamic damping is found for tilted mounted module under high wind speed. Compared to vertical displacement, horizontal and torsional displacements of the module are insignificant. The estimated wind vibration coefficients mainly lies between 1.1-2.7.
Keywords: Cable supported photovoltaic module, Aeroelastic test, Aerodynamic damping,

1. GENERAL INSTRUCTIONS

To deal with climate change challenge and satisfy the fast growing global energy demand, solar energy as a clean and safe renewable energy source, has been widely used for power generation recent years. With rapid expansion of solar energy plants, a cable-supported photovoltaic (PV) system has received increasing attention due to its large span and good terrain adaptability. It can be used in fishing ground, hilly area, and tideland, where the traditional beam supported structure is difficult to apply. However, the cable system is usually susceptible to wind action due to its lightweight and low damping. Therefore, wind induced vibration (WIV) of the cable-supported PV system is one of the dominant factors for structural safety. Most of previous studies focused on the aerodynamic characteristics of PV systems mounted on the ground or building roofs, only few of them were concerned with the long-span cable-supported PV system. This study carried out wind tunnel tests on both aeroelastic and rigid models to investigate the WIV characteristics of the new system, and the effects of tilt angle, cable pretension and wind speeds on the WIV response and aerodynamic damping were explained. Considering the load amplification effect caused by the fluctuating wind actions, wind vibration coefficient was derived when aiming to providing useful guidance for wind-resistant design of a cable-supported PV system.

2. WIND TUNNEL TEST OVERVIEW

The wind tunnel tests were conducted in the ZD-1 boundary layer wind tunnel at Zhejiang University, China. The geometry scale ratio was set to 1:10. A uniform wind field with a turbulence

intensity of 10% was used for the tests. The top and side views of the model are shown in Fig 1(a) and (b), respectively. The test wind azimuths(θ) varies from 0° to 180° with an interval of 15° as shown in Fig 1(a) and (c).

2.1. Aeroelastic test

During the aeroelastic test, two laser displacement meters were installed under the middle span (i.e. P4) and quarter span (i.e. P2) of the PV system to record the vertical displacement, as shown in Fig 1(b). The models with tilt angle α= 0° and 10° and initial pretension F=120N and 150N were adopted for test, respectively. The wind speed U increases from 5 to10 m/s during the test.

2.2. Wind pressure test

The rigid model with tilt angles of 0° and 10° were tested under wind speed of about 10 m/s. The reference point is selected at the height of 0.4 m. The wind pressures on the upper and lower surfaces of the PV module were measured simultaneously at a sampling frequency of 312.5 Hz.

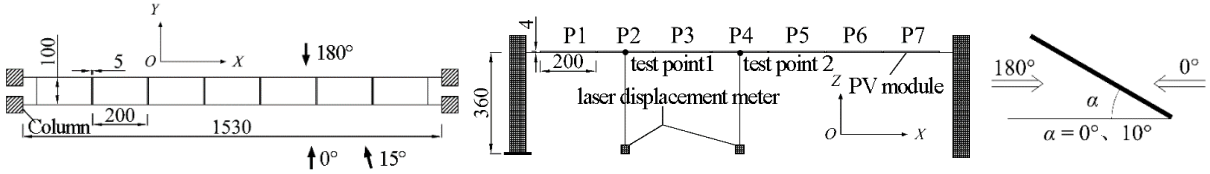

(a) Top view (b) Side view (c) test wind azimuth

Figure 1. Details of the test model and wind azimuth

3. TEST RESULTS

3.1. Wind-induced vertical vibration of PV modules with different tilt angles

For PV modules with α=0° and 10°, the Root Mean Square (RMS) of the vertical displacements (Z_{rms}) under F=150 N and U=5 m/s are given in Fig 2. It shows that the vertical vibration at α=10° is significantly higher than that at α=0°, and the maximum vertical response appears at the wind azimuth of 0° or 180°.

3.2. Effect of cable pretension and wind speed on WIV

The change rate of the RMS of vertical displacements, denoted as ΔZ, is introduced to show the influence of pretention on WIV. It can determined as

$$\Delta Z = \frac{Z_{120}\text{-}Z_{150}}{Z_{120}} \quad (1)$$

Where Z_{120} and Z_{150} are the RMS of the vertical displacement for the cases of F= 120N and 150N, respectively. For α=0° and 10°, ΔZ of midspan point P4 at U=5 and 10 m/s is presented in Fig 3. When the pretension is reduced from 150N to 120N, the average growth rate of the vertical response at α=0° is about 20% under both wind speeds, while that at α=10° is only about 10%, indicating the effect of pretension on the vertical structural stiffness is limited for the tilted mounted PV system. For α=10° and F=150 N, Fig 4 shows variation of Z_{rms} with wind speeds. It can be found that the vertical vibration increases almost linearly with the square of wind speed for the tilted mounted PV system.

3.3. Aerodynamic damping

The measured vibration data are first decomposed using variational modal decomposition to obtain the eigen-mode vectors. Then, the total damping ratio ξ_i of the PV system is identified using the Hilbert transform combined with random reduction technique. By subtracting inherent structural

damping ratio from total damping ratio derives aerodynamic damping ratio ξ_a. Fig 5 shows the variation of ξ_a with wind speed under wind azimuths of 0° and 180°, respectively. It can be found that the aerodynamic damping generally shows an decreasing trend with increase of wind speed(U). At wind azimuth of 180°, negative aerodynamic damping is observed under wind speed of 10m/s for both pretension cases.

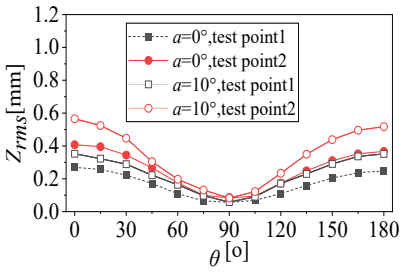

Figure 2. RMS of vertical displacement under different wind azimuth

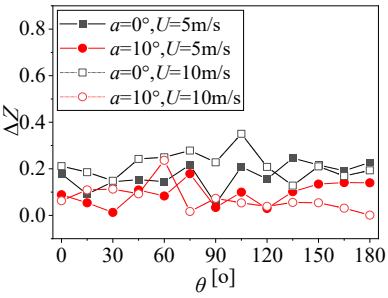

Figure 3. Variation of ΔZ with wind azimuth

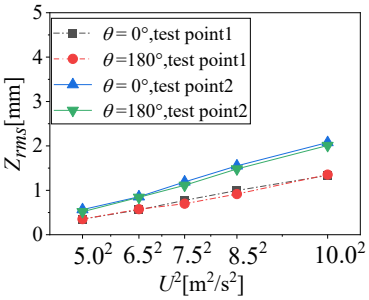

Figure 4. RMS of vertical displacements under different wind speeds (F=150N,a=10°)

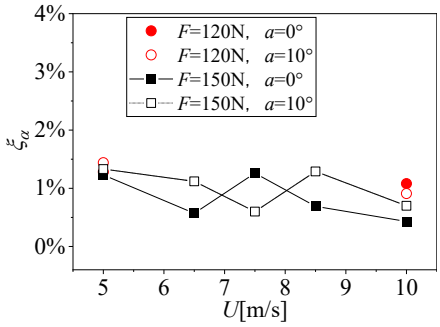

(a) θ=0°

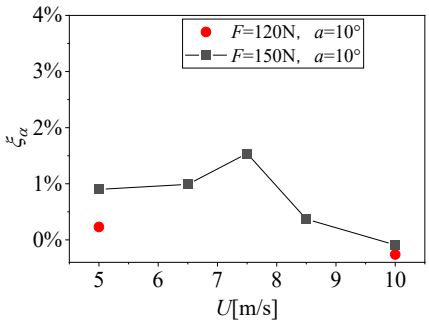

(b) θ=180°

Figure 5. Variation of aerodynamic damping with wind speed

4. THREE-DIMENSIONAL WIV OF PV MODULE

ANSYS finite element simulation is adopted to show the three-dimensional WIV of the cable supported PV system. The simulated vertical displacements are fist compared with the aeroelastic test results, and good agreement can be found. The results of torsional and horizontal responses for different tilt angles and wind speeds were given in Fig 7. It demonstrates that the torsional response is insignificant. Compared to the vertical displacement, the mean and RMS of the translational displacement are also much smaller, but they are larger than corresponding torsional responses. Therefore, it may be concluded that, for tested cable-supported PV system, the WIV is mainly contributed by vertical response, while the torsional response can be neglected.

5. WIND VIBRATION COEFFICIENT

The Load response correlation method (LRC) and multi-target equivalent method (extreme vertical responses of measuring points P4 and P2 are used as equivalent targets herein) were used to estimate static wind load which in turns derived the wind vibration coefficient (β) by dividing the mean wind load. Fig 8 shows the β of PV modules at α=10° and U=10m/s. The wind vibration coefficient increases from 1.1 at the side span to the maximum 2.7 at middle span. β under F=120

N is slightly higher than that under F=150 N.

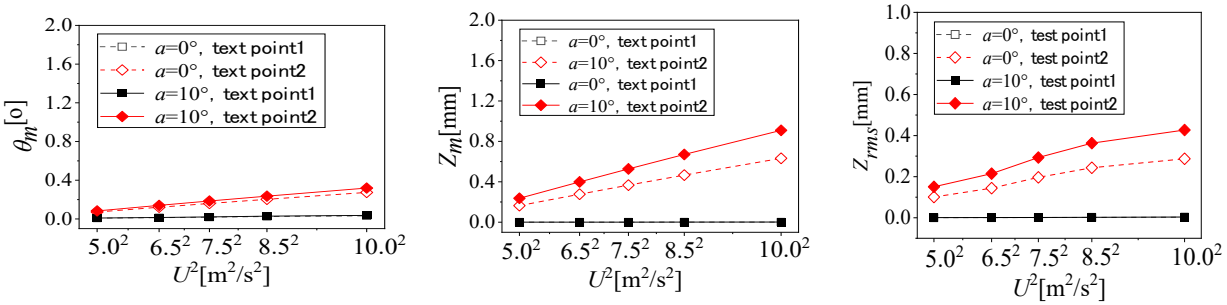

(a) mean angle of torsion (b) mean of translational displacement (c) RMS of translational displacement

Figure 7. Torsional and translational displacement responses under different wind speeds (F=150N, θ=0°)

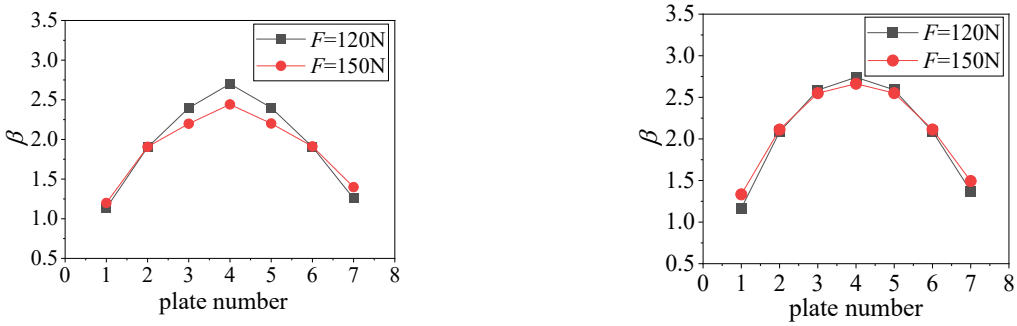

(a) θ=0° (b) θ=180°

Figure 8. Wind vibration coefficient of PV modules at α= 10°

6. CONCLUSION

(1) The vertical vibration of the cable-supported PV system increases with tilt angle. The maximum wind-induced vibration response occurs at the wind azimuth of 0° or 180° for both tilt angle cases.

(2) Increasing pretension may reduce the WIV, but for tilted mounted PV modules, such an effect is less significant. For the PV system with a tilt angle of 10°, the vertical displacement response increases almost linearly with the square of the wind speed.

(3) The WIV is mainly contributed by vertical response, while torsional response can be neglected.

(4) Negative aerodynamic damping may occur under high wind speed for tilted PV modules.

(5) The wind vibration coefficient mainly lies between 1.1 to 2.7.

REFERENCES

Baumgartner, F., et al, 2015. Solar ski lift PV carport and other solar wings cable based solutions. Proceedings of the 27th European Photovoltaic Solar Energy Conference, 24-28 Sept. 2012. Frankfurt, Canada, 4343-4347

Dragomiretskiy, K. and Zosso, D.,2014. Variational Mode Decomposition. Journal of IEEE Transactions on Signal Processing 62(3), 531-544.

Han J., et al, 2014. Structural modal parameter identification and damage diagnosis based on Hilbert-Huang transform. Journal of Earthquake Engineering and Engineering Vibration 13(1), 101-111.

Kasperski, M., Niemann, H. J., 1992. The LRC method: a general method of estimation unfavorable wind load distributions for linear and non-linear structures. Journal of wind Engineering and Industrial Aerodynamics 41(44),1753-1763.

Li, YX, et al, 2011. Multi-object resonant response equivalent static wind load of large-span roofs. Journal of Applied Mechanics and Materials 99, 1255-1258.